

A Study of Wire Sweep During Encapsulation of Semiconductor Chips

Se-Jin Han* and Yong-Jeong Huh**

*Sibley School of Mechanical and Aerospace Engineering, Cornell University

**School of Mechatronics Eng., Korea University of Technology and Education

Abstract : In this paper, methods to analyze wire sweep during the semiconductor chip encapsulation have been studied. The wire sweep analysis is used to analyze the deformation of bonding wires that connect the chip to the leadframe during encapsulation. The analysis is done using either analytical solutions or numerical simulation. The analytical solution is used for rough but fast calculation of wire sweep. The results from the numerical simulation are closest to the experimental results.

1. Introduction

This paper studies some of the problems that occur during the semiconductor chip encapsulation. The wire sweep analysis is used to analyze the deformation of bonding wires that connect the chip to the leadframe during encapsulation¹⁾. The analysis is done using either analytical solutions or numerical simulation. The analytical solution is used for rough but fast calculation of wire sweep. The numerical solution is used for more accurate calculation of wire sweep. The current analysis neglects the effect of wires on flow. C-MOLD Reactive Molding was used to calculate pressure in the cavity and ABAQUS was used to calculate the leadframe deformation. These simulation programs will be useful in designing encapsulation systems. For example, they can be used to design leadframe and wires. They can also be used to select optimal processing conditions, including mold temperature, filling time and curing time.

2. Wire Sweep Analysis

This study calculates wire sweep by considering wire deformation due to a viscous drag force of the fluid passing the wire during the filling stage of the encapsulation process. It is noted that wire deformation due to paddle or leadframe movement, possible wire deformation during the packing stage, as well as the effects of surface tension are neglected.

2.1 Global-Flow Analysis

The global-flow analysis is used to calculate the velocity, temperature and degree of cure distribution in the cavity by analyzing the flow in the pot, runners and cavities. In this study, C-MOLD Reactive Molding is used for global-flow analysis. For cavities that have leadframes inside, the cavity is divided by the leadframe into two parts (the upper and lower cavity). Each of these is treated as an independent cavity. This is equivalent to treating the leadframe as a solid wall with its temperature at the mold-wall temperature. The effect of the wire on flow has been neglected. This effect may be important when the number of wires used in the package is large. In generating a finite-element mesh, ideally, elements should be chosen so that the entire wire is contained within one element. Typically this would require too many elements. In a case where the velocity doesn't change much with planar location, a small number of elements can be used for wire sweep analysis.

Let's consider an example. The mold geometry for this example is shown in Fig. 1. This example considers the encapsulation of chips using transfer molding with an epoxy molding. The initial temperature of the melt is 85°C, the mold temperature is 180°C and the fill time is 12 seconds. The mold has twelve cavities; each cavity is 37×14×3.8 mm. There are 28 wires connecting the die and leadframe. The resulting predictions of the temperature and velocity distributions in the thickness direction at a center point of the cavity nearest to the

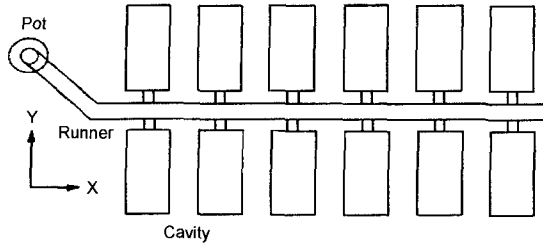


Fig. 1. A mold configuration for chip encapsulation.

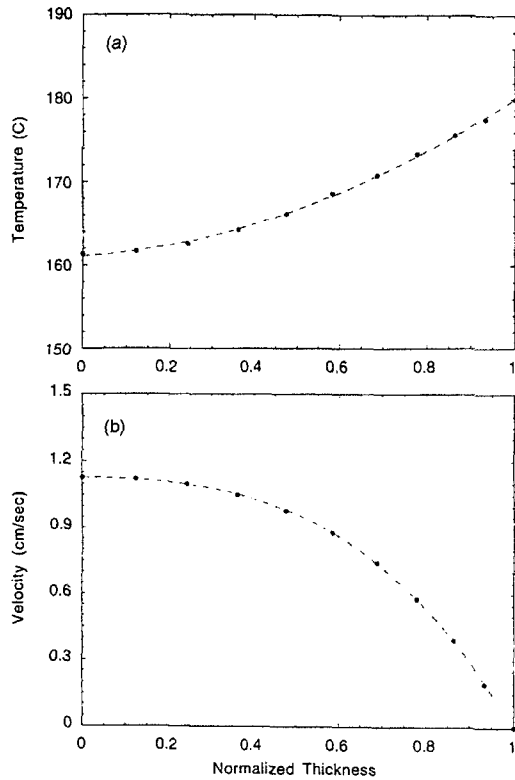


Fig. 2. (a) Temperature and (b) velocity distribution in the thickness direction at a central point of the cavity closest to the pot at 5 seconds of encapsulation.

pot, at 5 seconds, are shown in Fig. 2(a) and (b). These velocity and temperature distributions in the thickness direction can be approximated by third- and second-order polynomials as follows²⁾:

$$v = v_0 + (-9v_0 + 12v_B) + (8v_0 - 12v_B)(z/h)^3 \quad (1)$$

$$T = (1.5T_B - 0.5T_w) + (1.5T_w - 1.5T_B)(z/h)^2 \quad (2)$$

where v_0 is the velocity at the center of the cavity ($z=0$), v_B is the average velocity, T_w is the temperature at the

mold wall ($z=h$), T_B is the bulk temperature ("mixing-cup" temperature: weighted with local velocity) and z is the coordinate in the thickness direction. This fitting is shown as dash lines in the figure. Temperatures and velocities at any thickness location can be obtained from the above fitting.

2.2 Local-Flow Analysis

After having calculated the temperature and velocity distribution in the cavity from the global-flow analysis, we need to calculate the drag force exerted on the wire by solving the local flow field around the wire. Accurate calculation of the complicated geometry of the wire and leadframe would require a three-dimensional flow analyzer. It would also require non-isothermal and non-uniformly-curing analysis. However, use of such a detailed flow analyzer would require an enormous amount of computer resources. Therefore, a simplified analysis will be used to calculate the drag force. First, methods to calculate drag force on a cylinder for two-dimensional isothermal flow will be discussed. After that, methods to calculate the drag force on the wire of general shape at non-isothermal, non-uniformly-curing state will be discussed. Analytical and numerical methods will be used for this. The analytical solution is used for quick but approximate calculation of drag force. The numerical solution is used for more accurate calculation of drag force.

2.2.1 Drag-force Calculation on a cylinder for Two-dimensional Isothermal Flow

(1) Analytical Equation

Lamb's Model

This method assumes that the cavity walls are infinitely distant from the wire, thus neglecting effects of the walls on the drag force calculation. For Newtonian fluids, this approach calculates the drag force on the wire as follows³⁻⁴⁾:

$$D = \frac{C_D \rho U^2 d}{2} \quad (3)$$

$$C_D = \frac{8\pi}{Re[2.002 - \ln(Re)]} \quad (4)$$

$$Re = \frac{\rho U d}{\eta} \quad (5)$$

Where D is the drag force per unit length of the

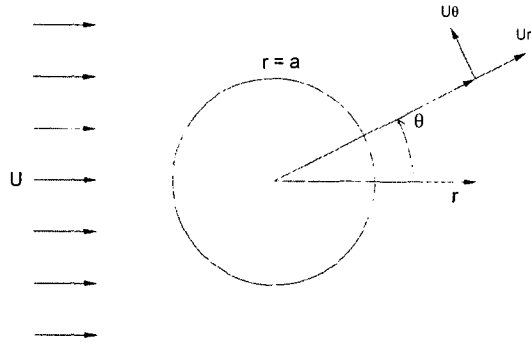


Fig. 3. Coordinate system used in Lamb's equation.

wire, d is the diameter of the wire and U, η, ρ are the undisturbed upstream velocity, viscosity and density, respectively, of the fluid passing the wire, which are seen in Fig. 3. This equation is valid for creeping flow ($Re \ll 1$).

Takaisi's Model

This method considers the effects of the cavity wall on the drag force. The calculation of the drag force on the wire is based on the following equation⁵⁾:

$$D = 4\pi\eta b_o \tag{6}$$

where

$$b_o = \frac{U}{\ln(h/a) - 0.9156 + 1.7243(a/h)^2} \tag{7}$$

where a is the radius of the wire and h is the half-gap thickness of the mold cavity.

This empirical equation is only valid for a Newtonian fluid under a creeping flow ($Re \ll 1$) condition; it was obtained by Takaisi(1956) by curve fitting experimental results for a rectangular cavity cross-section of h/a in the range of 20 to 200.

(2) Numerical Simulation

For non-newtonian fluids, we cannot use the above-mentioned methods. In this case, we need to use numerical analysis of the flow to calculate the drag force on the wire. In this study, analysis of a two-dimensional flow around a wire is carried out by solving the following set of equations(neglecting inertial effects):

$$\frac{\partial u}{\partial x} + \frac{\partial v}{\partial y} = 0 \tag{8}$$

$$\frac{\partial(\sigma_{xx} - p)}{\partial x} + \frac{\partial\sigma_{xy}}{\partial y} = 0 \tag{9}$$

$$\frac{\partial(\sigma_{xy})}{\partial x} + \frac{\partial(\sigma_{yy} - p)}{\partial y} = 0 \tag{10}$$

where, for a generalized Newtonian fluid⁶⁾.

$$\sigma_{xx} = 2\eta \frac{\partial u}{\partial x}, \sigma_{yy} = 2\eta \frac{\partial v}{\partial y}, \sigma_{xy} = \eta \left(\frac{\partial u}{\partial y} + \frac{\partial v}{\partial x} \right) \tag{11}$$

where η can be shear-rate, temperature and degree-of-cure dependent. For the present, however, we neglect non-isothermal and curing effects. Using the finite-element method with rectangular elements and a quadratic shape function for velocity and linear shape function for pressure, the Galerkin formulation results in the following set of matrices to solve for u, v and p ⁷⁾:

$$[K] \begin{Bmatrix} u \\ v \\ p \end{Bmatrix} = \begin{Bmatrix} R_u \\ R_v \\ 0 \end{Bmatrix} \tag{12}$$

where $[K]$ itself is a variable due to the shear-rate dependence of viscosity and where R_u and R_v arise from boundary conditions.

The above equations are solved iteratively until they converge, taking into account the non-linearity arising from the shear-rate dependence of viscosity. From the resulting shear stress and pressure along the wire, we can calculate the drag force per unit length on the wire by the following equation:

$$D = -\int_0^{2\pi} \tau_{y\theta} \sin \theta a d\theta - \int_0^{2\pi} p \cos \theta a d\theta \tag{13}$$

where $\tau_{y\theta}$ is the shear stress in the circumferential direction and a is the radius of the wire.(See polar coordinates defined in Fig. 3.

2.2.2 Drag-force Calculation on Wires in a Chip

Using the drag force calculation method for two-dimensional isothermal flow on a cylinder, the drag force on a wire will be calculated as explained below for the general case. In doing so, the following assumptions will be made:

(i) It is noted that the length of the wire used in the semiconductor chip is usually much greater than the

diameter of the wire, so we may treat the flow at a specific point along the wire as locally two-dimensional. Therefore, we calculate the drag force at a point of the wire from the two-dimensional flow analysis with the velocity at that point obtained from the global-flow analysis as the uniform upstream fluid velocity.

(ii) Regarding the temperature and degree of cure, the drag force at a point of the wire will be calculated by assuming that the temperature and degree of cure is uniform in the flow field with values of temperature and degree of cure at that point obtained from the global flow analysis. This assumption has been made because fluid near the wire will affect the drag force more than fluid far from the wire.

(iii) The wire will be assumed to be at the center of the cavity even though, in the actual case, the wire is not at the center of the cavity. This assumption has been made because Taneda (1964) showed that drag force on the wire is relatively constant unless the wire is close to the wall.

These approximations will make the results less accurate compared to a rigorous three-dimensional, non-isothermal and non-uniformly-curing flow analysis, but they are made to calculate results at a reasonable cost. The detailed steps of the local-flow analysis are as follows:

(1) The drag force on a cylinder which has the same diameter as the wire used in the chip encapsulation can be calculated either by analytical method or by numer-

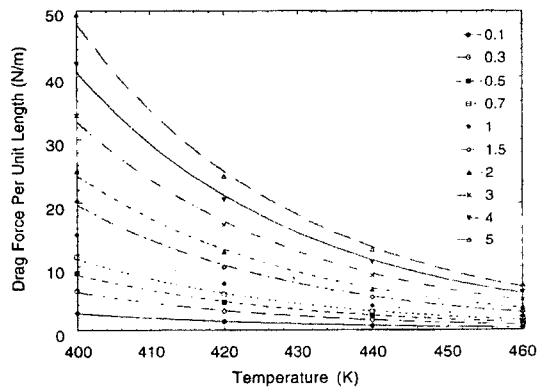


Fig. 4. Drag force on a wire at different temperatures and velocities (Numbers inside the plot denote the fluid velocity in cm/sec).

ical method. In using the numerical methods, if we perform numerical analysis for each temperature and velocity along the wire, it would take too much time. To save computational time, the drag force at some velocities and temperatures within the range encountered during encapsulation can be calculated. By fitting these drag forces calculated at some velocities and temperatures, drag force at any velocity and temperature can be obtained from the fitting equation. One example of the calculated drag forces is shown in Fig. 4. The results indicate that the drag force can be fitted by the following empirical equation:

$$D = (a_0 v^{a_1}) * \text{EXP}((b_0 + b_1 v) * T) \quad (14)$$

where v and T are the velocity and temperature of fluid passing the wire and a_0 , a_1 , b_0 , b_1 are fitting constants. This is because once the viscosity starts to rise due to curing, the viscosity will rise very rapidly. Therefore, most filling processes are designed to be completed before any appreciable rise in viscosity takes place. In a case where the viscosity rise due to curing is not negligible, its effect can be included approximately by the following equation:

$$D = (a_0 v^{a_1}) * \text{EXP}((b_0 + b_1 v) * T) * \left(\frac{\alpha_g}{\alpha_g - \alpha} \right)^{(c_1 + c_2 \alpha)} \quad (15)$$

where α is the degree of cure, c_1 and c_2 are fitting constants. The values of parameters in the above equation are functions of the viscosity of the fluid and the ratio of half-gap thickness to wire radius (h/a).

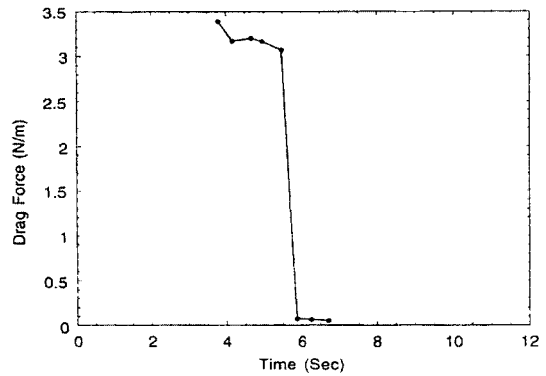


Fig. 5. Drag force as a function of time.

(2) Making use of the predicted bulk temperature and bulk velocity at each instant during the filling stage obtained from global-flow analysis, the drag force on the wire is calculated by using equation¹⁵⁾. Choose a time at which the resulting calculated drag force on the wire is maximum. An example of such a calculated drag force versus time is shown in Fig. 5. For this case, the drag force is at its maximum at about 3.8 seconds, and the velocity and temperature distributions in the gap at this time will be used in the wire sweep calculation.

(3) Calculate the drag force on the wire at a particular point along the wire by using equation¹⁵⁾ with the temperature and velocity at that point obtained from global flow analysis corresponding to the time obtained in step (2).

2.3. Wire Deformation Calculation

2.3.1 Analytical Solutions

Some analytical solutions on the wire deformation are available if we assume linear elastic behavior of the wire. Two examples are shown below.

(1) Nguyen's Formula

From reference 8, when $L \gg H$, the wire deformation in the direction of load P can be calculated by the following equation⁸⁾:

$$\delta = \frac{PH^3}{24GI_p} + \frac{PL^3}{24EI} \tag{16}$$

where δ is the wire deformation, P is the load, H is the height, L is the length of the wire, G is the shear modulus, E is the elongational modulus, I_p is the polar moment of inertia and I is the moment of inertia.

(2) Circular Arch

Another form of approximate solution can be obtained by representing the wire geometry as a part of circular arch (Fig. 6). In this case the deformation of the wire can be found from the following equation⁹⁾:

$$\delta = \delta_A + \Theta_A R \sin x + \Psi_A R (1 - \cos x) + \frac{M_A R^2}{EI} F_1 + \frac{T_A R^2}{EI} F_2 + \frac{V_A R^3}{EI} F_3 - \frac{w R^4}{EI} F_{a13} \tag{17}$$

The definition of all the constants in the above equation can be found from reference 9.

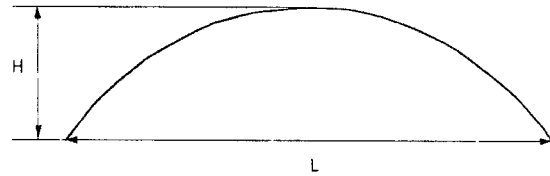


Fig. 6. Representation of wire geometry as a circular arch

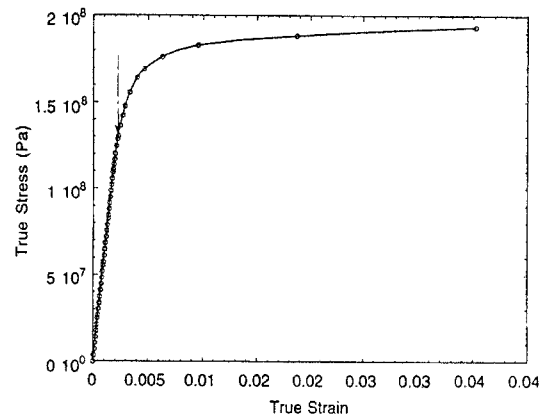


Fig. 7. Procedures used for wire sweep analysis in this study.

2.3.1 Calculation Using ABAQUS

In general, the wire deformation is not elastic, the load may have arbitrary distribution and the deformation can be big. In this case we need to use numerical simulation for an accurate wire deformation calculation. The commercial software product ABAQUS can be used for this purpose. When the wire deforms, the velocity and temperature at the new position may be different from the original values. Using the new velocity and temperature at the new position of the wire, calculate the deformation of the wire. Repeat this process until convergence. For the mechanical property of the wire, use the mechanical property of the wire at the encapsulation temperature (shown in Fig. 7).

2.4 Comparison of Calculated and Experimental Results

Three different methods of wire sweep calculation have been done as shown in Fig. 8. Fig. 9 shows wire sweep data experimentally measured and calculated as outlined in Fig. 8. The values are for a wire which lies normal to the flow direction. It also gives wire sweep data calculated by various methods.

In Fig. 9, "Numerical" denotes the results obtained

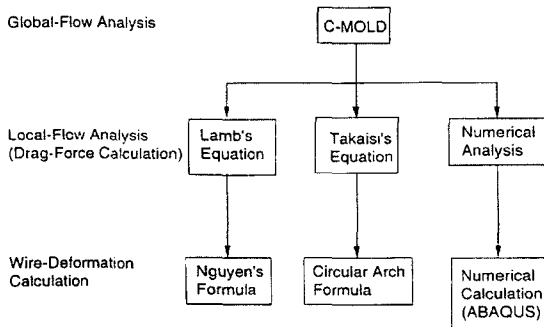


Fig. 8. Comparison of wire sweep values experimentally measured and calculated by various methods.

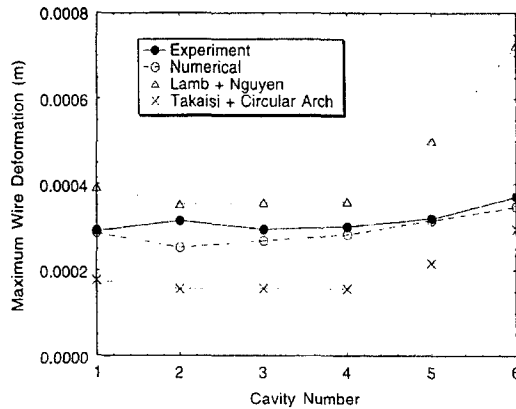


Fig. 9. Comparison of wire sweep values experimentally measured and calculated by various methods.

when the numerical simulation was used to calculate the drag force and the wire deformation; "Lamb+Nguyen" denotes the results obtained when the drag force was calculated by Lamb's equation and wire deformation was calculated by Nguyen's method; "Takaisi+Circular Arch" denotes the results obtained when the drag force was calculated by Takaisi's method and Circular Arch formula was used for the wire deformation calculation. As can be seen from Fig. 9, the results from the numerical simulation are closest to the experimental results²⁾. The Lamb+Nguyen method gives consistently higher values and the Takaisi+Circular Arch method gives lower values.

3. Conclusion

In this paper, methods to analyze wire sweep during

the semiconductor chip encapsulation have been studied. The wire sweep analysis is used to analyze the deformation of bonding wires that connect the chip to the leadframe during encapsulation.

The analysis is done using either analytical solutions or numerical simulation. The analytical solution is used for rough but fast calculation of wire sweep and the numerical solution is used for more accurate calculation of wire sweep.

Three different methods of wire sweep calculation have been evaluated. The Lamb+Nguyen method gives consistently higher value than experimentally measured one, but in contrast the Takaisi+Circular Arch method gives lower value than experimentally measured one. And the results obtained from the numerical simulation show a good agreement with experimental values.

References

1. Manzione, L.T., *Plastic Packaging of Microelectronic Devices*, Van Nostrand Reinhold, New York, 1990.
2. Han, S., A Study on Plastic Encapsulation of Semiconductor Chips, Ph.D Dissertation, Cornell University, 1994.
3. White, F. M., *Viscous Fluid Flow*, McGraw-Hill, New York, 1974.
4. Nguyen, L.T., "Wire bond behavior during molding operations of electronic packages", *Polymer Engineering and Science*, V.28, pp926-943, 1988
5. Takaisi, Y., "Note on the drag on a circular cylinder moving with low speeds in a viscous liquid between two parallel walls", *J. Physical Society of Japan*, v.11, p.1059, 1956.
6. Bird, R. B., Armstrong, R. C. and Hassager, O., *Dynamics of Polymeric Liquids*, vol. 1, Wiley-Interscience, New York, 1987.
7. Huebner, K. H. and Thornton, E. A., *The Finite Element Method for Engineers*, John Wiley & Sons, New York, 1982.
8. Nguyen, L. T., Danker, A., Santhiran, N. and Shervin, C. R., "Flow Modeling of Wire Sweep during Molding of Integrated Circuits", *ASME Winter Annual Meeting*, p.27, 1992.
9. Young, W. C., *Roark's Formulas for Stress and Strain*, pp.326-328, McGraw-Hill Book Company, New York, 1975